

# Deep Face Fuzzy Vault: Implementation and Performance

Christian Rathgeb, Johannes Merkle, Johanna Scholz, Benjamin Tams, Vanessa Nesterowicz

**Abstract**—Deep convolutional neural networks have achieved remarkable improvements in facial recognition performance. Similar kinds of developments, e.g. deconvolutional neural networks, have shown impressive results for reconstructing face images from their corresponding embeddings in the latent space. This poses a severe security risk which necessitates the protection of stored deep face embeddings in order to prevent from misuse, e.g. identity fraud.

In this work, an unlinkable improved deep face fuzzy vault-based template protection scheme is presented. To this end, a feature transformation method is introduced which maps fixed-length real-valued deep face embeddings to integer-valued feature sets. As part of said feature transformation, a detailed analysis of different feature quantisation and binarisation techniques is conducted using features extracted with a state-of-the-art deep convolutional neural network trained with the additive angular margin loss (ArcFace). At key binding, obtained feature sets are locked in an unlinkable improved fuzzy vault. For key retrieval, the efficiency of different polynomial reconstruction techniques is investigated. The proposed feature transformation method and template protection scheme are agnostic of the biometric characteristic and, thus, can be applied to virtually any biometric features computed by a deep neural network.

For the best configuration, a false non-match rate below 1% at a false match rate of 0.01%, is achieved in cross-database experiments on the FERET and FRGCv2 face databases. On average, a security level of up to approximately 28 bits is obtained. This work presents the first effective face-based fuzzy vault scheme providing privacy protection of facial reference data as well as digital key derivation from face.

**Index Terms**—Biometric Template Protection, Biometric Cryptosystem, Fuzzy Vault Scheme, Face Recognition.

## I. INTRODUCTION

FACE recognition technologies are employed in many personal, commercial, and governmental identity management systems around the world. In a face recognition system, a *reference face image* is captured at enrolment; the face is detected, pre-processed, and a feature vector is extracted which is stored as *reference template*. At the time of authentication, a *probe face image* is captured, processed in the same way, and compared against a reference template of a claimed identity (verification) or up to all stored reference templates (identification). For a long period of time, handcrafted feature extractors, e.g. Local Binary Patterns [1] and Gabor filters [2], were predominately used. Said methods apply texture descriptors locally and aggregate extracted features into an overall face descriptor. A large variety of such systems has

The authors are with secunet Security Networks AG, Essen, Germany. C. Rathgeb is also with the Hochschule Darmstadt, Germany. J. Scholz and V. Nesterowicz are also with the Ruhr-Universität Bochum.  
E-mail: {name}.{lastname}@secunet.com

been proposed in the scientific literature, see [3], [4]. In contrast, state-of-the-art face recognition technologies utilise deep learning and massive training datasets to learn rich and compact representations of faces [5], [6]. The recent developments in Deep Convolutional Neural Networks (DCNNs) have led to breakthrough advances in facial recognition accuracy, surpassing human-level performance [7], [8].

Privacy regulations, e.g. the General Data Protection Regulation (GDPR) [9], generally classify biometric templates as sensitive data; in order to prevent from misuse, stored biometric reference data must be protected. It is well-known that traditional encryption methods are unsuitable for protecting biometric data, due to the natural intra-class variance of biometric characteristics, in particular the face. More precisely, biometric variance prevents from a biometric comparison in the encrypted domain, *i.e.* analogous to password hashing. Consequently, the use of conventional cryptographic methods would require a decryption of protected biometric data prior to the comparison. In contrast, *biometric template protection* [10]–[12] enables a comparison of biometric data in the encrypted domain and hence a permanent protection of biometric data. Biometric template protection schemes use auxiliary data to obtain pseudonymous identifiers from unprotected biometric data. Biometric comparisons are then performed via pseudonymous identifiers while unprotected biometric data are discarded [13]. Biometric template protection methods are commonly categorised as *cancelable biometrics* and *biometric cryptosystems*. The latter type of template protection techniques further allows for the derivation of digital keys from protected biometric templates, *e.g.* fuzzy commitment [14] and fuzzy vault scheme [15]. Thereby, biometric cryptosystems offer a biometrics-based solution to key management.

In the past decades, numerous biometric template protection schemes have been proposed for various biometric characteristics, including face, see subsection II-B. This large amount of research notwithstanding, face-based biometric cryptosystems have received relatively little attention in biometric research. This may be explained by the limited biometric performance achieved by face recognition during the high time of research on biometric template protection (approximately in the early 2000s). Obviously, privacy protection and sizes of derived keys are theoretically upper bounded by the biometric performance of the underlying recognition system, in particular its false match rate [16], [17]. As mentioned before, the biometric performance of face recognition has significantly improved in the recent past such that low false match rates are achieved at practical false non-match rates. This motivates the (re-)investigation of face-based biometric cryptosystems.

In this work, an unlinkable improved face fuzzy vault-based cryptosystem is proposed which enables the protection of deep face embeddings, hereafter referred to as *deep face representations*, as well as key derivation thereof. For this purpose, a biometric characteristic-agnostic feature transformation is introduced which transforms a real-valued feature vector to a set of integer features. This transformation is based on a three-stage process involving a feature quantisation, a feature binarisation, and a feature set mapping step. To the best of the authors' knowledge this is the first unlinkable improved fuzzy vault scheme adapted to deep face recognition. Combinations of different quantisation and binarisation methods are investigated in a comprehensive performance evaluation. Evaluations are conducted in cross-database experiments on two publicly available face databases using an open-source deep face recognition system. Moreover, a detailed performance and security evaluation of the proposed face-based fuzzy vault is given where multiple configurations of the proposed feature transformation are investigated. In addition, various decoding strategies and their runtime are analysed for key retrieval. It is worth noting that the proposed feature transformation method and template protection scheme can be applied to any features computed by deep neural networks. Therefore, the presented face fuzzy vault can be easily extended to a multi-biometric scheme using feature-level fusion, whereby a very high level of security can be achieved.

The remainder of this work is organised as follows: section II revisits related works. The proposed fuzzy vault scheme is described in detail in section III and experiments based on deep face representations are presented and discussed in section IV. Concluding remarks are given in section V.

## II. BACKGROUND AND RELATED WORK

Biometric template protection has been an active field of research for more than two decades. For comprehensive surveys on this topic the interested reader is referred to [10]–[12], [18]. Cancelable biometrics employ transforms in signal or feature domain which enable a biometric comparison in the transformed (encrypted) domain [19]. In contrast, the majority of biometric cryptosystems binds a key to a biometric feature vector resulting in a protected template. Biometric comparison is then performed indirectly by verifying the correctness of a retrieved key [20]. Alternatively, homomorphic encryption has frequently been suggested for biometric template protection [21]. Homomorphic encryption makes it possible to compute operations in the encrypted domain which are functionally equivalent to those in the plaintext domain and thus enables the estimation of certain distances between protected biometric templates. The requirements on biometric template protection schemes are defined in ISO/IEC IS 24745 [13]:

- **Unlinkability:** the infeasibility of determining if two or more protected templates were derived from the same biometric instance, *e.g.* face. By fulfilling this property, cross-matching across different databases is prevented.
- **Irreversibility:** the infeasibility of reconstructing the original biometric data given a protected template and its corresponding auxiliary data. With this property fulfilled, the privacy of the users' data is increased, and

TABLE I: Properties of template protection categories.

| Template protection category | Unlinkability | Irreversibility | Renewability | Performance preservation | Efficient comparison | Key derivation |
|------------------------------|---------------|-----------------|--------------|--------------------------|----------------------|----------------|
| Cancelable biometrics        | ✓             | ✓               | ✓            | (✓)                      | ✓                    |                |
| Biometric cryptosystems      | ✓             | ✓               | ✓            | (✓)                      | (✓)                  | ✓              |
| Homomorphic encryption       | ✓             | ✓               | ✓            | ✓                        | (✓)                  |                |

additionally the security of the system is increased against presentation and replay attacks.

- **Renewability:** the possibility of revoking old protected templates and creating new ones from the same biometric instance and/or sample, *e.g.* face image. With this property fulfilled, it is possible to revoke and reissue the templates in case the database is compromised, thereby preventing misuse.
- **Performance preservation:** the requirement of the biometric performance not being significantly impaired by the protection scheme.

Table I gives an overview of the aforementioned categories of biometric template protection and their properties w.r.t. the above criteria as well as key derivation and efficient biometric comparison. In contrast to homomorphic encryption, the vast majority of works on cancelable biometrics and biometric cryptosystems reports a performance gap between protected and original (unprotected) systems [12]. Cancelable biometrics usually employ a biometric comparator similar or equal to that of unprotected biometric systems. Thereby, cancelable biometrics are expected to maintain the comparison speed of the unprotected system which makes them also suitable for biometric identification [22]. Biometric cryptosystems may need more complex comparators. Similarly, homomorphic encryption usually requires higher computational effort. In contrast to cancelable biometrics and homomorphic encryption, biometric cryptosystems enable the binding and retrieval of digital keys.

Some research efforts and standardisation activities have been devoted to establishing metrics for evaluating the aforementioned properties of biometric template protection schemes, *e.g.* in [23]–[27]. Nonetheless, additional specific cryptanalytic methods may be necessary to precisely estimate the security/privacy protection achieved by a particular template protection scheme. Moreover, the result of such an evaluation also depends on the biometric data to which the template protection system is applied. This makes a comparison of published results difficult and sometimes misleading.

The following subsection discusses the necessity of feature type transformations for biometric template protection (subsection II-A). Subsequently, the most relevant works on face-based biometric template protection are briefly summarised (subsection II-B). Afterwards, the fuzzy vault scheme is revisited in detail (subsection II-C).

### A. Feature Type Transformation

Common feature representations have been established for templates of different biometric characteristics, *e.g.* minutiae sets for fingerprints. However, biometric template protection schemes, in particular biometric cryptosystems, require templates in a distinct type of feature representation, *e.g.* fixed-length binary strings for the fuzzy commitment scheme. In order to make biometric templates compatible to a template protection scheme, a feature type transformation may be necessary [28]. This is particularly the case for multi-biometric template protection where fusion should be performed at the feature level to achieve high security levels [29].

Focusing on face, biometric templates frequently consist of fixed-length integer- or real-valued feature vectors, *e.g.* aggregated descriptors of facial regions or deep face representations extracted by DCNNs. To protect facial data in template protection schemes which take binary bit strings as input, numerous binarisation techniques have been proposed [28]. A recent benchmark of popular binarisation schemes was presented in [30]. Additionally, techniques for adapting the intra-class variance of face feature vectors to error correction capabilities of biometric cryptosystems have been proposed, *e.g.* in [31]. Recently, researchers have suggested to train DCNNs to generate compact binary strings, commonly referred to as Deep Hashing [32], [33]. Such techniques have already been adapted to obtain binary face representations for biometric template protection, *e.g.* in [34], [35]. To obtain feature sets from binary face templates, various researchers have proposed to divide binary vectors into small bit-chunks and convert those directly to their decimal representation, *e.g.* in [36].

### B. Face Template Protection

In 2001, Ratha *et al.* [37] proposed the first cancelable face recognition system using image warping to transform biometric data in the image domain. Another popular cancelable transformation of face images based on random convolution kernels was presented in [38]. In contrast to [37], this approach employs a fundamentally reversible distortion of the biometric signal based on some random seed which later coined the term “biometric salting”. The majority of published cancelable face recognition schemes applies transformations in the feature domain [19]. Over the past years, numerous feature transformations have been proposed in order to construct face-based cancelable biometrics, *e.g.* BioHashing [39], BioTokens [40], and Bloom filters [41]. Recently, feature transformations have been specifically designed for DCNNs, *e.g.* random subnet-work selection [35]. Analyses of some popular cancelable face recognition systems have uncovered security gaps, *e.g.* in [42]–[45], and already led or are expected to lead to (continuous) improvements of such schemes.

Regarding biometric cryptosystems, the fuzzy commitment scheme [14] and the fuzzy vault scheme [15] represent widely used cryptographic primitives. Both schemes enable an error-tolerant protection of (biometric) data by binding them with a secret, *i.e.* key. Binarised face feature vectors have been protected through the fuzzy commitment scheme in various

scientific publications, *e.g.* in [31], [35], [46], [47]. However, it was shown that the fuzzy commitment scheme can not effectively protect against correlation attacks [48]. In contrast, only a few works have employed the fuzzy vault scheme for face template protection (see subsection II-C). It is worth mentioning that some template protection approaches combine concepts of cancelable biometrics with those of biometric cryptosystems resulting in hybrid schemes [11].

For a long time, homomorphic encryption has been considered as impractical for biometric template protection due to its computational workload. However, in the last years, homomorphic encryption has been applied effectively to face recognition where practical processing times could be achieved on commodity hardware [49]–[51]. Depending on the used homomorphic cryptosystem, different feature type transformations might be required [52].

More recently, so-called privacy enhancing face recognition has been proposed by various researchers, *e.g.* in [53], [54]. The common goal of these approaches is to train a DCNN for face recognition in a way that suppresses demographic information within deep face representations, *e.g.* sex or age. Thus, privacy enhancing face recognition partially fulfills requirements of biometric template protection.

### C. Fuzzy Vault Scheme

The fuzzy vault scheme was introduced by Juels and Sudan [15], [55] and enables protection and error-tolerant verification with feature sets. It was suggested for the protection of fingerprint minutiae sets in [56]. Building upon this preliminary analysis, a series of implementations for minutiae-based fingerprint fuzzy vaults was proposed [57], [58]. A useful guide for constructing a fuzzy vault scheme is provided in [59]. Different security analyses have found that the original fuzzy vault scheme is vulnerable to a certain kind of linkage attack, *i.e.* the correlation attack [60], [61]. This conflicts with the above mentioned requirement of unlinkability as well as irreversibility. Dodis *et al.* [62] presented an improved version of the fuzzy vault scheme which generates much smaller records. It was later shown that the aforementioned linkage attack can be effectively prevented in the improved fuzzy vault scheme [63], [64].

Until now, the fuzzy vault scheme has been applied to various physiological as well as behavioural biometric characteristics, *e.g.* iris [65] and online signatures [66]. Additionally, fuzzy vault schemes utilising multi-biometric fuzzy vaults have been presented, *e.g.* in [67], [68].

Regarding the face, only a few early works applied the fuzzy vault scheme. Within those schemes, handcrafted feature vectors are extracted and different feature type transformations are employed to obtain feature sets. Moreover, various decoding startegies were used. All published approaches were evaluated on rather small databases, *e.g.* in [69], [70]. Further, the majority of schemes reported impractical performance rates in terms of recognition accuracy in particular false match rates, *e.g.* in [71]. High false match rates make those schemes vulnerable to false accept attacks which were rarely considered. The false accept security which is derived from a system’s false match

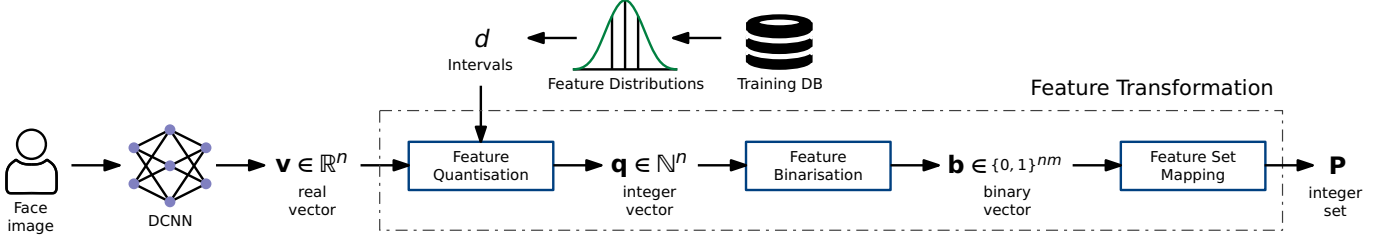


Fig. 1: Overview of the proposed feature transformation process.

rate provides a good approximation of the actual security. In contrast, some works report brute-force security, *e.g.* 41 bits in [69], which is usually a clear overestimate of the actual security considering corresponding recognition rates. The work in [36] represents a notable exception, reporting a false accept security for a face-based fuzzy vault. Obviously, published approaches on face-based fuzzy vault systems did not employ DCNN-based face recognition which represent the current state-of-the-art. A more detailed overview face-based fuzzy vault schemes and reported biometric performance as well as security rates is provided in subsection IV-E.

For constructing a fuzzy vault-based cryptosystem, a practical decoding strategy is needed. To this end, a Reed-Solomon decoder [72] has been proposed in the original fuzzy vault scheme [15], [55]. In [57], the repeated use of a Lagrange-based decoder has been suggested and adopted for other implementations [58], [64]. A reasonable trade-off between decoding time and verification performance can be achieved using a Guruswami-Sudan-based decoder [73]. In this work, these strategies are considered for key retrieval (see subsection III-B).

### III. FUZZY VAULT FOR DEEP REPRESENTATIONS

DCNNs are usually trained using *differentiable* loss functions, *e.g.* Euclidean distance. Consequently, deep face representations are represented as fixed-length real-valued vector  $\mathbf{v} \in \mathbb{R}^n$ . This particularly applies to state-of-the-art face recognition systems. In the feature transformation step of the proposed system, deep (face) representations are transformed to integer-valued feature sets (subsection III-A). Subsequently, key binding and retrieval is performed in an unlinkable improved fuzzy vault scheme (subsection III-B).

#### A. Feature Transformation

An overview of the feature transformation process is shown in figure 1. It comprises the following three main steps:

1) *Feature Quantisation*: In the feature quantisation step, a real-valued feature vector  $\mathbf{v} = (v_i)_{i=1}^n, v_i \in \mathbb{R}$  is mapped to a quantised integer-valued feature vector  $\mathbf{q} = (q_i)_{i=1}^n, q_i \in \mathbb{N}_0$  of same size. For this purpose, the probability densities of all  $n$  feature elements are estimated. Based on its obtained probability density, the feature space of each feature element is then divided into  $d = 2^x$  integer-labelled intervals. Each element of the feature vector is then mapped to an integer number representing the corresponding interval on its support. Two quantisation schemes are applied:

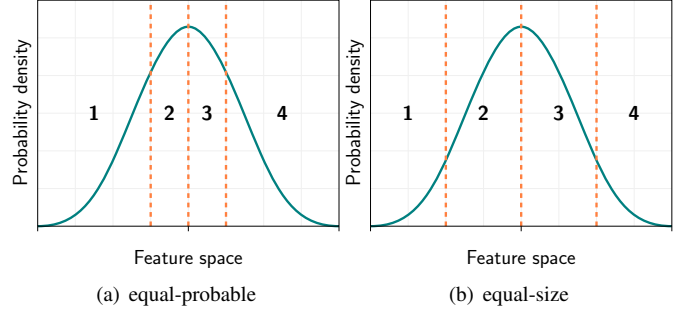


Fig. 2: Example of quantisation of feature space in four intervals.

- **Equal-probable intervals**: the feature space is divided into intervals containing equal population probability mass.
- **Equal-size intervals**: the feature space is divided into intervals of equal size.

An example of both quantisation schemes is illustrated in figure 2. The division of feature spaces of feature elements into intervals is determined based on a training database. Note that equal-size intervals can also be estimated directly given the feature space ranges.

2) *Feature Binarisation*: In the binarisation step, the quantised feature vector  $\mathbf{q}$  is mapped to a binary feature vector  $\mathbf{b} \in (b_i)_{i=1}^{nm}, b_i \in \{0, 1\}$ . Precisely, each quantised feature element  $q_i$  (represented as integer) is mapped to a binary string  $b_i$  of length  $m$ . Subsequently, all binary strings are concatenated to produce the final binary feature representation of size  $nm$ . The dissimilarity of two such templates can be then computed using the Hamming distance. The following binarisation schemes are considered:

- **Boolean**: The feature spaces are quantised into  $d = 2$  sub-spaces (*i.e.* the resulting binary string is a single 0 or 1). In this simple scheme, the size of the quantised feature vector is maintained, *i.e.*  $m = 1$ .
- **DBR** (Direct Binary Representation): In this scheme, the quantised feature elements are converted directly into their base-2 (binary) representations. The resulting binary vector is of size  $nm$  with  $m = \log_2(d)$ .
- **BRGC** (Binary Reflected Gray Code [74]): The binarisation is done in a way that the Hamming distance between codewords resulting from successive decimal values is always 1. The size of the binary vector is equal to that of DBR.
- **LSSC** (Linearly Separable Subcode [75]): A more recent

TABLE II: Binarisation methods with four intervals.

| Quantisation Interval | Method  |     |      |      |         |
|-----------------------|---------|-----|------|------|---------|
|                       | Boolean | DBR | BRGC | LSSC | One-hot |
| 1                     | 0       | 00  | 00   | 000  | 0001    |
| 2                     | 1       | 01  | 01   | 001  | 0010    |
| 3                     | -       | 10  | 11   | 011  | 0100    |
| 4                     | -       | 11  | 10   | 111  | 1000    |

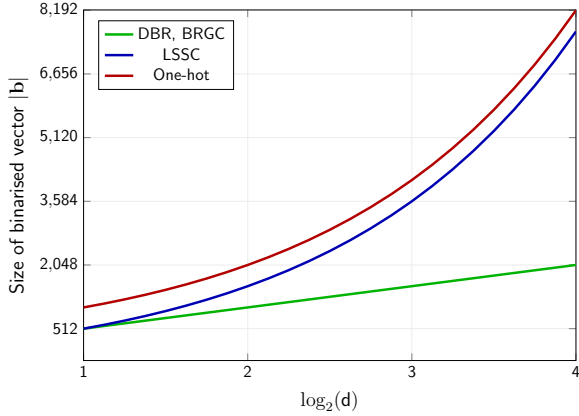


Fig. 3: Relation between used number of intervals and sizes of the binarised feature vectors for a quantised feature vector of size 512.

approach, in which the distances between two binary values are equal to the  $L1$  norm between the corresponding quantised values. Compared to the previous schemes the size of the binary feature vector is significantly larger with  $m = d - 1$ .

- **One-hot:** In this scheme, the length of the binary representation is equal to that of the used intervals, *i.e.*  $m = d$ . In each binarised value, only one bit is set to 1 which corresponds to the interval index resulting from the quantisation step (one-hot encoding). When applied to all feature elements, this results in a sparse binary feature vector. Note that the Hamming distance of such one-hot binary vectors corresponds to that of quantised feature vectors which is 1 for differing feature elements regardless of their distance.

Table II shows an example for the binarisation methods described above with four intervals. A decrease in entropy density can be observed for the LSSC and the one-hot binarisation methods since theoretically only  $2^{n \log_2(d)}$  different binary feature vectors can be generated for all binarisation methods. Intuitively, there exists a trade-off between the ability to obtain better separation, representation sparsity, and the required length of the binary vector. For a quantised vector of size 512, the relation between the number of intervals and the corresponding binarised vector is plotted for the different binarisation methods in figure 3.

3) **Feature Set Mapping:** In the last step of the feature transformation process, the binary feature vector  $\mathbf{b}$  is mapped to a feature set  $\mathbf{P}$ . The features in  $\hat{\mathbf{P}}$  are interpreted as elements of a finite field  $\mathbf{F}$ . This feature set consists of all indexes of 1s in the binary vector, *i.e.*  $\mathbf{P} = \{i | b_i = 1\}$ . The size of the feature set is equal to the Hamming weight of the binary vector,  $|\mathbf{P}| = HW(\mathbf{b})$ . This mapping of binary

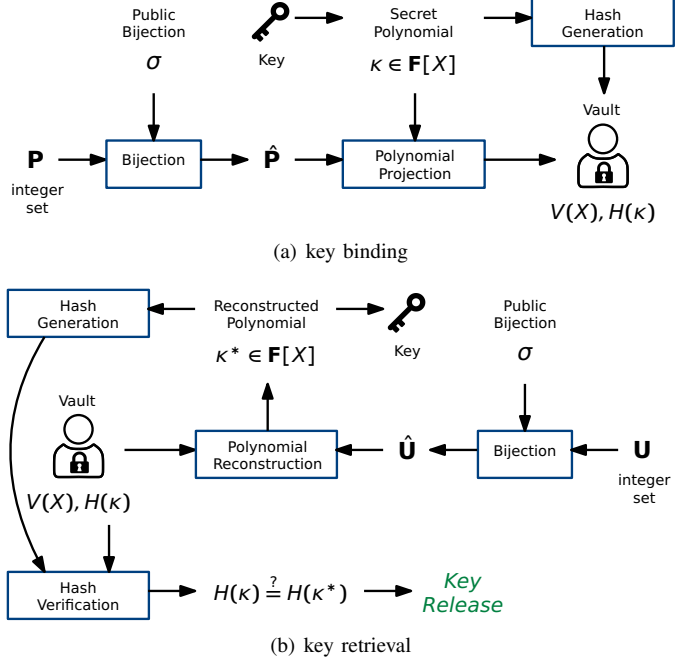


Fig. 4: Overview of key binding and key retrieval.

features to feature sets is different from those proposed in published works which usually map binary chunks to their decimal representation, *e.g.* in [36]. In contrast, the proposed mapping is less sensitive to single bit flips and is therefore expected to obtain higher biometric performance in a fuzzy vault scheme.

### B. Key Binding and Retrieval

The key binding (enrolment) and retrieval (verification) processes are illustrated in figure 4. In the first step of the binding process, a secret polynomial  $\kappa \in \mathbf{F}[X]$  of degree smaller than  $k$  is chosen and the hash  $H(\kappa)$  is stored. A record-specific but public bijection  $\sigma : \mathbf{F} \rightarrow \mathbf{F}$  is applied to the feature set  $\mathbf{P}$ , in order to re-map the elements of  $\mathbf{P}$ ,  $\hat{\mathbf{P}} = \sigma(\mathbf{P}) = \{\sigma(v) | v \in \mathbf{P}\}$ . To avoid additional data storage, it is suggested to use  $H(\kappa)$  as seed to generate  $\sigma$ . This first step is performed as a countermeasure to the attack proposed in [63], see subsection IV-D. It is important to note that the application of a public bijection does not affect the biometric performance of the fuzzy vault scheme.

The next step is performed based on the improved fuzzy vault scheme [62]. Feature elements are encoded by a monic polynomial of degree  $t = |\hat{\mathbf{P}}|$ . The features in  $\hat{\mathbf{P}}$  are interpreted as elements of a finite field  $\mathbf{F}$ ,  $|\mathbf{F}| = \rho$ , and bound to the secret polynomial  $\kappa$  by estimating  $V(X) = \kappa(X) + \prod_{v \in \hat{\mathbf{P}}} (X - v)$ . The pair  $(V(X), H(\kappa))$  is the final vault record. The elements of  $\hat{\mathbf{P}}$  can be represented with exactly  $\log_2(nm)$  bits. The size of the vault increases with  $t$  and is upper bounded by  $nm \log_2(nm)$  bits.

At key retrieval, a probe feature set  $\mathbf{U} \subset \mathbf{F}$  is computed. By evaluating the polynomial  $V(X)$  on its elements, a set of pairs  $\{(x, V(x)) | x \in \mathbf{U}\}$  is obtained. Since  $V(x) = \kappa(x)$  for  $x \in \hat{\mathbf{P}}$ , the pairs  $(x, V(x))$  with  $x \in \mathbf{U} \cap \hat{\mathbf{P}}$  lie on the function

curve of the secret polynomial  $\kappa(X)$ ; these pairs are referred to as genuine. If the number  $\omega$  of genuine points is at least  $k$ , it is possible to reconstruct the polynomial  $\kappa$  from  $\mathbf{U}$ . The correctness of  $\kappa$  can be verified, *e.g.* by using the hash value  $H(\kappa)$ . It may, however, not be feasible to reconstruct  $\kappa$  in case  $\omega \geq k$ . For the used feature extractor and the proposed feature transformation the unlocking set is expected to be sufficiently large to successfully recover  $\kappa$ , see section IV.

The following polynomial reconstruction strategies are considered in this work:

1) *Iterated Lagrange Strategy*: To reconstruct  $\kappa$  from  $\mathbf{U}$ ,  $k$  pairs are selected from  $\mathbf{U}$  and the unique polynomial  $\kappa^*$  of degree smaller than  $k$  that interpolates them is estimated. If all  $k$  selected pairs are genuine, then  $\kappa^* = \kappa$  which can be verified by observing  $H(\kappa^*) = H(\kappa)$ . If not all  $k$  selected pairs are genuine, then most likely  $H(\kappa^*) \neq H(\kappa)$  and the procedure is repeated until  $H(\kappa^*) = H(\kappa)$ . This procedure is guaranteed to, eventually, reconstruct the secret polynomial  $\kappa$  if  $\omega \geq k$ . For a single step the success probability is equal to

$$p_L(u, \omega, k) = \binom{\omega}{k} \cdot \binom{u}{k}^{-1}. \quad (1)$$

Depending on the parameters  $u$ ,  $k$ , and  $\omega$ , the iterated Lagrange strategy can become too costly and hence impractical as it may require a huge amount of iterations before  $\kappa$  is recovered.

2) *Reed-Solomon Strategy*: Alternatively, a Reed-Solomon decoder, *e.g.* see [72], is capable of recovering  $\kappa$  from  $\mathbf{U}$  efficiently (by means of deterministic polynomial time) in case  $\omega \geq (u+k)/2$ . However, this class of algorithms will fail to recover  $\kappa$  from  $\mathbf{U}$  for  $\omega < (u+k)/2$ . To obtain a decoding mechanism which can deal with these cases, it is suggested to randomly select a  $c$ -sized subset  $\mathbf{U}_0 \subset \mathbf{U}$  where  $|\mathbf{U}| \geq c \geq k$ . Subsequently, the Reed-Solomon decoder can be applied to  $\mathbf{U}_0$ , and, if successfully revealing  $\kappa^*$  with  $H(\kappa^*) = H(\kappa)$ , output the recovered polynomial; otherwise, this procedure is repeated until predefined number of iterations is reached. This procedure will succeed eventually if  $\omega \geq (c+k)/2$  which improves upon the bound  $\omega \geq (u+k)/2$  since  $c \leq u$ . The success probability for a single step is equal to

$$p_{RS}(u, \omega, k, c) = \binom{u}{c}^{-1} \sum_{j=\lceil(c+k)/2\rceil}^{\min(\omega, c)} \binom{\omega}{j} \cdot \binom{u-\omega}{c-j}. \quad (2)$$

The Reed-Solomon decoding strategy is expected to significantly improve upon the iterated Lagrange method while it may still be too costly for a practical implementation. It is noteworthy that a Reed-Solomon decoder can be viewed as a special case of a Guruswami-Sudan decoder.

3) *Guruswami-Sudan Strategy*: By employing a Guruswami-Sudan list decoder [73], the bound  $\omega \geq (u+k)/2$  can be significantly improved. Provided that  $\omega > \sqrt{u \cdot (k-1)}$ , this algorithm can potentially recover  $\kappa^1$ . While the Guruswami-Sudan decoder can be time-consuming in practice if one aims at recovering up

<sup>1</sup>As a list decoder, the Guruswami-Sudan algorithm returns a list of candidate polynomials. From these, the correct can be easily determined by checking its hash value.

to  $u - \sqrt{u \cdot (k-1)}$  errors, the computational efficiency can be traded-off against the number of correctable errors by an additional parameter referred to as multiplicity. This algorithm may represent a significant improvement compared to a Reed-Solomon decoder.

An Guruswami-Sudan strategy will recover  $\kappa$  from  $\mathbf{U}$  in a single step with probability

$$p_{GS}(u, \omega, k, c) = \binom{u}{c}^{-1} \sum_{j=\lceil\sqrt{c \cdot (k-1)}\rceil}^{\min(\omega, c)} \binom{\omega}{j} \cdot \binom{u-\omega}{c-j}. \quad (3)$$

This strategy is expected to outperform the iterated Lagrange as well as the Reed-Solomon strategies.

The Guruswami-Sudan decoding method could be optimised by iteratively increasing the multiplicity until  $\kappa$  is successfully recovered or a maximum number of iterations is reached. Moreover, it can be combined with one of the aforementioned decoding strategies as suggested in [67]. However, these optimizations are not deployed in our implementation.

#### IV. APPLICATION TO FACE AND EVALUATION

The following subsection describes the experimental setup for applying the proposed fuzzy vault to deep face representations (subsection IV-A). Subsequently, the performance of the different variants of quantisation and binarisation methods are evaluated in a first experiment (subsection IV-B). In the second experiment, the proposed feature transformation is applied based using the best performing quantisation and binarisation schemes and the biometric performance of the deep face fuzzy vault scheme is estimated using the different decoding strategies (subsection IV-C). In the last experiment, a corresponding security and runtime analysis is presented (subsection IV-D). Finally, the proposed system is compared against other works (subsection IV-E).

##### A. Software and Databases

For the extraction of deep face representations, the original implementation of the widely used ArcFace approach [76] is employed. This DCNN has been trained using the additive angular margin loss and achieves competitive recognition performance on various challenging datasets. In this work, we used the pre-trained model LResNet100E-IR, ArcFace@ms1m-refine-v2 published in the model zoo of the original ArcFace implementation<sup>2</sup>. This model takes input images of size  $112 \times 112$  pixels and extracts deep face representations of 512 floats. For the image preprocessing (alignment, cropping and scaling), we closely followed the ArcFace implementation, but replaced the MTCNN face detector by the face and landmark detection of the dlib library [77].

Experiments are conducted in a cross-database setting using manually selected subsets of the publicly available FERET [78] and FRGCv2 [79] databases. That is, the training process in which feature distributions are estimated to determine the quantization parameters, is conducted on the FERET database and the evaluation is performed on the FRGCv2 database and

<sup>2</sup><https://github.com/deepinsight/insightface>

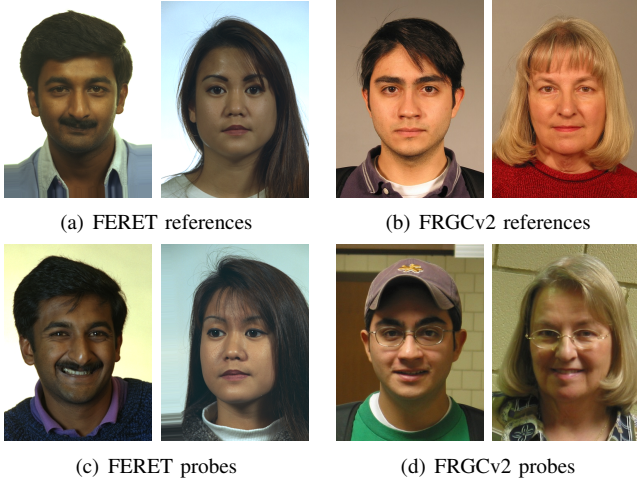


Fig. 5: Examples of reference and probe images of the used databases.

TABLE III: Overview of face image subsets from the FERET and FRGCv2 face databases: amount of subjects, corresponding reference and probe images as well as resulting number of mated and non-mated comparisons (“f” and “m” denote female and male, respectively).

| Database | Subjects (f/m) | Images    |       | Comparisons |           |
|----------|----------------|-----------|-------|-------------|-----------|
|          |                | Reference | Probe | Mated       | Non-Mated |
| FERET    | 529 (200/329)  | 529       | 791   | 791         | 147,712   |
| FRGCv2   | 533 (231/302)  | 984       | 1,726 | 3,298       | 144,032   |

vice versa. Reference and probe images were chosen with the aim of simulating a cooperative authentication scenario where the enrolment process has been performed in a controlled environment. Precisely, reference images of both databases largely fulfill the requirements defined by International Civil Aviation Organization (ICAO) in [80], in particular frontal pose and neutral expression. In contrast, probe images exhibit variations in pose, expression, focus and illumination. If possible, probe images were preferably chosen from different acquisition sessions in order to obtain a realistic scenario. Examples of probe and reference images of both face image subsets are depicted in figure 5. Generally, the FRGCv2 subset contains less constrained images and is considered as more challenging, compared to the FERET subset as well as databases used in previously published works, see table VII. Table III lists the number of subjects, corresponding reference and probe images, as well as the resulting mated and non-mated comparisons.

### B. Binariation Methods

In the first experiment, combinations of quantisation and binarisation methods described in section III-A are benchmarked against the baseline system. Feature elements of deep face representations extracted from images of the FERET and FRGCv2 databases were found to lie in the range  $[-0.3, 0.3]$ , which was used as basis for estimating equally-sized intervals. In the baseline system, comparison scores between pairs of deep face representations are obtained by estimating their

TABLE IV: Performance results in terms of EER (in%) |  $d'$  for different binarisation methods on both databases.

| Method   | Intervals<br>$d$ | Training: FRGCv2                 |                                 | Training: FERET                   |                                  |
|----------|------------------|----------------------------------|---------------------------------|-----------------------------------|----------------------------------|
|          |                  | Evaluation: FERET<br>equal-prob. | Evaluation: FERET<br>equal-size | Evaluation: FRGCv2<br>equal-prob. | Evaluation: FRGCv2<br>equal-size |
| Baseline | –                | 0.0                              | 9.9                             | 0.0                               | 9.4                              |
| Boolean  | 2                | 0.0   9.7                        | 0.0   9.5                       | 0.003   8.2                       | 0.003   8.2                      |
|          | 4                | 0.0   7.2                        | 0.0   8.9                       | 0.003   7.5                       | 0.003   7.6                      |
|          | 8                | 0.0   6.6                        | 0.0   6.6                       | 0.02   7.1                        | 0.03   6.3                       |
| DBR      | 16               | 0.0   6.4                        | 0.001   5.6                     | 0.03   6.7                        | 0.03   6.0                       |
|          | 4                | 0.0   8.1                        | 0.0   9.2                       | 0.002   7.4                       | 0.002   8.0                      |
|          | 8                | 0.0   6.3                        | 0.0   8.8                       | 0.01   6.6                        | 0.07   8.0                       |
| BRGC     | 16               | 0.0   5.8                        | 0.0   6.4                       | 0.003   6.2                       | 0.04   6.5                       |
|          | 4                | <b>0.0   10.2</b>                | 0.0   9.2                       | <b>0.001   9.1</b>                | 0.002   8.0                      |
|          | 8                | <b>0.0   10.3</b>                | 0.0   9.6                       | <b>0.07   9.3</b>                 | 0.07   8.8                       |
| LSSC     | 16               | <b>0.0   10.3</b>                | 0.0   9.8                       | <b>0.07   9.3</b>                 | 0.07   9.1                       |
|          | 4                | 0.0   7.0                        | 0.0   8.7                       | 0.001   7.1                       | 0.002   7.6                      |
|          | 8                | 0.0   5.3                        | 0.0   6.0                       | 0.006   5.9                       | 0.01   5.8                       |
| One-hot  | 16               | 0.0   4.6                        | 0.11   4.0                      | 0.18   5.1                        | 0.19   4.6                       |

Euclidean distance. Biometric performance is evaluated in terms of False Non-Match Rate (FNMR) and False Match Rate (FMR) [81]. In particular the Equal Error Rate (EER), *i.e.* the operation point where FNMR = FMR, is reported. Further, a measure of decidability ( $d'$ ) [82] calculated as

$$d' = \frac{|\mu_g - \mu_i|}{\sqrt{\frac{1}{2}(\sigma_g^2 + \sigma_i^2)}} \quad (4)$$

is reported, where  $\mu_g$  and  $\mu_i$  represent the means of the mated and the non-mated comparison trials score distributions and  $\sigma_g$  and  $\sigma_i$  their standard deviations, respectively. Larger decidability values indicate better separability of mated and non-mated comparison scores.

Table IV gives an overview of the obtained results. It can be observed that the baseline system achieves a perfect separation between mated and non-mated scores on both databases while generally lower decidability measures are obtained for the FRGCv2 database (which confirms that this database is more challenging). Further, it can be seen that the Boolean binarisation method reduces the discriminativity of deep face representations, in particular on the FRGCv2 database. Neither the DBR nor the BRGC binarisation schemes improve upon the Boolean method. When using more intervals the performance generally decreases for these binarisation schemes.

In contrast to the aforementioned binarisation schemes, the biometric performance achieved by the LSSC method is close to that of the baseline system. Best results are obtained when dividing the feature space into equally probable intervals. Here, the biometric performance generally improves with the number of intervals into which the feature space is divided. However, biometric performance quickly converges such that a no significant improvements are observable when using more than 8 intervals. Note that in some cases this method even shows a better decidability than the baseline system.

The one-hot method obtains the worst biometric performance. Similar to the DBR and BRGC schemes, for this binarisation approach performance rates decrease if a larger number of intervals is used.

Based on this first experiment it can be concluded that the LSSC-based binarisation scheme with equally probable inter-

TABLE V: Performance results in terms of FNMR | FMR (in %) for the fuzzy vault scheme using Lagrange (LG), Reed-Solomon (RS), and Guruswami-Sudan (GS) decoding strategies on both databases.

| Intervals<br><i>d</i> | Degree<br><i>k</i> | Training: FRGCv2, Test: FERET |             |             | Training: FERET, Test: FRGCv2 |               |               |
|-----------------------|--------------------|-------------------------------|-------------|-------------|-------------------------------|---------------|---------------|
|                       |                    | LG                            | RS          | GS          | LG                            | RS            | GS            |
| 4                     | 16                 | 0.0   99.05                   | 0.0   99.70 | 0.0   100.0 | 0.0   99.23                   | 0.0   99.79   | 0.0   100.0   |
|                       | 32                 | 0.002   0.33                  | 0.0   99.05 | 0.0   100.0 | 0.30   0.48                   | 0.0   99.29   | 0.0   100.0   |
|                       | 48                 | 3.26   0.0                    | 0.0   97.48 | 0.0   100.0 | 33.54   0.001                 | 0.0   97.95   | 0.0   100.0   |
|                       | 64                 | 24.04   0.0                   | 0.0   94.11 | 0.0   100.0 | 85.86   0.0                   | 0.0   95.05   | 0.0   100.0   |
|                       | 96                 | 72.99   0.0                   | 0.0   77.41 | 0.0   100.0 | 99.57   0.0                   | 0.0   80.58   | 0.0   100.0   |
|                       | 256                | 99.99   0.0                   | 0.0   0.06  | 0.0   58.94 | 99.99   0.0                   | 0.0   0.28    | 0.0   63.50   |
|                       | 288                | 99.99   0.0                   | 0.0   0.004 | 0.0   13.75 | 100.0   0.0                   | 0.0   0.035   | 0.0   18.36   |
|                       | 320                | 100.0   0.0                   | 0.0   0.001 | 0.0   1.033 | 100.0   0.0                   | 0.061   0.006 | 0.0   2.277   |
|                       | 352                | 100.0   0.0                   | 0.0   0.0   | 0.0   0.031 | 100.0   0.0                   | 0.819   0.001 | 0.0   0.154   |
|                       | 384                | 100.0   0.0                   | 0.0   0.0   | 0.0   0.001 | 100.0   0.0                   | 4.639   0.001 | 0.061   0.009 |
|                       | 416                | 100.0   0.0                   | 1.263   0.0 | 0.0   0.0   | 100.0   0.0                   | 13.06   0.001 | 1.637   0.001 |
|                       | 448                | 100.0   0.0                   | 2.273   0.0 | 0.758   0.0 | 100.0   0.0                   | 33.08   0.0   | 10.21   0.001 |
|                       | 480                | 100.0   0.0                   | 7.449   0.0 | 2.146   0.0 | 100.0   0.0                   | 59.15   0.0   | 31.71   0.0   |
|                       | 512                | 100.0   0.0                   | 16.41   0.0 | 8.586   0.0 | 100.0   0.0                   | 82.01   0.0   | 62.85   0.0   |
| 8                     | 16                 | 0.0   99.99                   | 0.0   100.0 | 0.0   100.0 | 0.0   99.99                   | 0.0   100.0   | 0.0   100.0   |
|                       | 32                 | 0.0   2.750                   | 0.0   100.0 | 0.0   100.0 | 0.008   3.520                 | 0.0   100.0   | 0.0   100.0   |
|                       | 48                 | 0.996   0.003                 | 0.0   100.0 | 0.0   100.0 | 13.41   0.005                 | 0.0   100.0   | 0.0   100.0   |
|                       | 64                 | 11.26   0.0                   | 0.0   100.0 | 0.0   100.0 | 68.41   0.0                   | 0.0   100.0   | 0.0   100.0   |
|                       | 96                 | 60.45   0.0                   | 0.0   99.99 | 0.0   100.0 | 98.72   0.0                   | 0.0   100.0   | 0.0   100.0   |
|                       | 512                | 100.0   0.0                   | 0.0   18.84 | 0.0   99.99 | 100.0   0.0                   | 0.0   24.23   | 0.0   99.99   |
|                       | 576                | 100.0   0.0                   | 0.0   4.657 | 0.0   99.37 | 100.0   0.0                   | 0.0   7.728   | 0.0   99.52   |
|                       | 640                | 100.0   0.0                   | 0.0   0.723 | 0.0   87.63 | 100.0   0.0                   | 0.0   1.774   | 0.0   89.68   |
|                       | 704                | 100.0   0.0                   | 0.0   0.070 | 0.0   44.72 | 100.0   0.0                   | 0.0   0.283   | 0.0   50.51   |
|                       | 768                | 100.0   0.0                   | 0.0   0.004 | 0.0   9.033 | 100.0   0.0                   | 0.0   0.041   | 0.0   13.08   |
|                       | 832                | 100.0   0.0                   | 0.0   0.001 | 0.0   0.697 | 100.0   0.0                   | 0.030   0.006 | 0.0   1.666   |
|                       | 896                | 100.0   0.0                   | 0.0   0.0   | 0.0   0.019 | 100.0   0.0                   | 0.424   0.002 | 0.0   0.130   |
|                       | 960                | 100.0   0.0                   | 0.126   0.0 | 0.0   0.001 | 100.0   0.0                   | 2.941   0.001 | 0.061   0.009 |
|                       | 1024               | 100.0   0.0                   | 0.631   0.0 | 0.0   0.0   | 100.0   0.0                   | 9.096   0.001 | 1.092   0.001 |

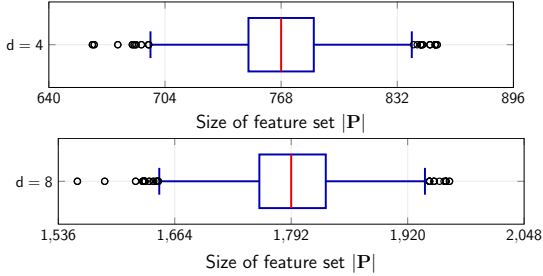


Fig. 6: Box plots of feature set sizes across both databases.

vals is the most suitable method as it maintains the biometric performance of the baseline system. This confirms the findings in [30], where similar results were reported for other DCNN-based face representations. Therefore, only this binarisation approach with up to 8 intervals will be considered for the construction of the fuzzy vault scheme in the subsequent experiments.

### C. Fuzzy Vault Construction and Decoding Strategy

Firstly, the sizes of feature sets are estimated. For equal probable intervals the expected size of a feature set is  $E(|P|) = |\mathbf{b}|/2$  with  $|\mathbf{b}| = n(d-1)$  for the LSSC method and  $n = 512$  for the used ArcFace system. Figure 6 depicts box plots of distributions of feature set sizes for different numbers of intervals across both used databases. It can be observed that set sizes are narrowly-distributed around their expected values with only a few mild outliers. In fact, feature set sizes approximate a binomial distribution  $B(n(d-1); 0.5)$ , *i.e.* the probability of feature set sizes which are considerably smaller

or larger than the expected value quickly diminishes. This narrow distribution of feature set sizes implies that the maximum observed vault size will be significantly below the theoretical maximum which in turn reduces storage requirement. From figure 6, it can be observed that set sizes quickly increase with the number of used intervals, *c.f.* figure 3.

Table V gives an overview of obtained biometric performance in terms of FNMR and FMR for the fuzzy vault scheme employing different decoding strategies on both databases. For the Lagrange decoder  $2^{16}$  decoding attempts are performed where best performance rates are obtained at rather small polynomial degrees of approximately 32 and 48 for using 4 and 8 quantisation intervals, respectively. The Reed-Solomon decoder achieves competitive performance rates at higher polynomial degrees, *i.e.* approximately 320 for 4 intervals and 900 for 8 intervals. Comparable performance rates are obtained for applying the Guruswami-Sudan decoding with a multiplicity of 1, although at even higher polynomial degrees. Specifically, on the FERET database, a perfect separation between mated and non-mated decoding attempts is maintained, *e.g.* for  $d = 4$  and  $k = 416$ . For  $d = 4$  and  $k = 384$ , a FNMR of 0.06% at a FMR<0.01% is achieved on the more challenging FRGCv2 database. In summary, it can be observed that the use of a Reed-Solomon and a Guruswami-Sudan decoding strategies yield highest recognition accuracies.

### D. Security and Runtime Analysis

Security is measured in terms of False Accept Security (FAS). As mentioned earlier, compared to the FAS, the Brute-Force Security (BFS) tends to significantly overestimate the effective security of a fuzzy vault scheme [64]. The BFS

TABLE VI: Performance in relation to security in terms of GMR (in %) | FAS (in bits) and decoding time in terms of  $t_g$  |  $t_i$  (in ms) for the fuzzy vault scheme using the Guruswami-Sudan decoding strategy on both databases.

| Intervals<br>$d$ | Degree<br>$k$ | Training: FRGCv2,<br>Test: FERET | Training: FERET,<br>Test: FRGCv2 | Decoding time |
|------------------|---------------|----------------------------------|----------------------------------|---------------|
| 4                | 320           | 100.00   12.1                    | 100.00   11.0                    | 82.5   68.2   |
|                  | 336           | 100.00   14.5                    | 100.00   12.8                    | 80.1   68.1   |
|                  | 352           | 100.00   17.2                    | 100.00   14.9                    | 80.2   68.4   |
|                  | 368           | 100.00   20.3                    | 99.97   16.9                     | 80.8   68.8   |
|                  | 384           | 100.00   21.7                    | 99.94   19.0                     | 81.9   70.1   |
|                  | 400           | 100.00   23.0                    | 99.52   19.9                     | 82.7   70.5   |
|                  | 416           | 100.00   24.4                    | 98.36   21.7                     | 83.4   69.1   |
|                  | 432           | 99.75   25.7                     | 95.18   21.7                     | 83.9   69.2   |
|                  | 448           | 99.24   27.1                     | 89.78   21.7                     | 84.7   70.9   |
|                  | 464           | 98.61   28.4                     | 81.57   22.7                     | 85.1   70.3   |
|                  | 480           | 97.85   29.8                     | 68.28   23.7                     | 83.6   71.2   |
|                  | 496           | 95.33   31.1                     | 52.64   24.7                     | 83.3   70.4   |
|                  | 512           | 91.41   32.5                     | 37.14   25.6                     | 83.0   70.2   |
| 8                | 1008          | 100.00   26.9                    | 99.49   23.3                     | 401.0   359.3 |
|                  | 1024          | 100.00   27.9                    | 98.91   24.4                     | 402.3   360.2 |
|                  | 1040          | 99.87   28.9                     | 98.12   24.5                     | 403.6   364.1 |
|                  | 1056          | 99.87   29.8                     | 96.60   24.5                     | 406.0   363.5 |
|                  | 1072          | 99.62   30.8                     | 95.00   24.6                     | 413.0   364.5 |
|                  | 1088          | 99.62   31.8                     | 92.94   24.6                     | 419.6   365.5 |
|                  | 1104          | 99.50   32.8                     | 90.27   24.7                     | 417.2   374.0 |
|                  | 1120          | 98.86   33.7                     | 86.66   25.7                     | 419.5   367.4 |
|                  | 1136          | 98.61   34.7                     | 82.29   25.8                     | 423.4   369.3 |
|                  | 1152          | 98.23   35.7                     | 76.90   25.8                     | 426.3   376.1 |
|                  | 1168          | 97.85   36.7                     | 69.89   25.9                     | 429.6   373.9 |
|                  | 1184          | 97.10   37.6                     | 62.64   25.9                     | 432.0   378.3 |
|                  | 1200          | 95.83   38.6                     | 55.25   25.9                     | 442.9   397.1 |

usually increases with the degree of the secret polynomial. Precisely, for the proposed system the minimum BFS observed (in bits) was similar to the size of the polynomial, *i.e.*  $\min(\text{BFS}) \approx k$ . Therefore, a more realistic measure can be derived from the FMR. An attacker can iteratively simulate non-mated verification attempts until the vault is unlocked thereby running a false-accept attack; within each simulated attempt, the probability of success equals the FMR. The FAS is estimated as,

$$l \cdot \log(0.5) / \log(1 - \text{FMR}) \quad (5)$$

where  $l$  is the average amount of operations for a non-mated verification attempt. Precisely, the FAS defines the number of operations that an attacker requires to succeed with a probability of 50% (alternatively, the FAS could be estimated as  $l/\text{FMR}$ , *i.e.* the expected number of steps until an attack succeeds. From table V, it can be observed that, for any polynomial degree, the Guruswami-Sudan decoding strategy yields the highest FMR. Therefore, it is reasonable to assume that an attacker would use the Guruswami-Sudan algorithm during a false-accept attack. The amount of operations needed for the Guruswami-Sudan decoding algorithm is measured relatively to the Lagrange method. Precisely, we express the effort of an attack by the number of Lagrange interpolations that would (roughly) result in the same computational time. For different polynomial degrees the computational times required by the used decoding strategies was empirically estimated. Note that this results in a rather conservative measure, since a single Lagrange interpolation for the used degrees  $k$  is expected to be more time consuming than a decryption attempt within a classical cryptographic method, *e.g.* AES.

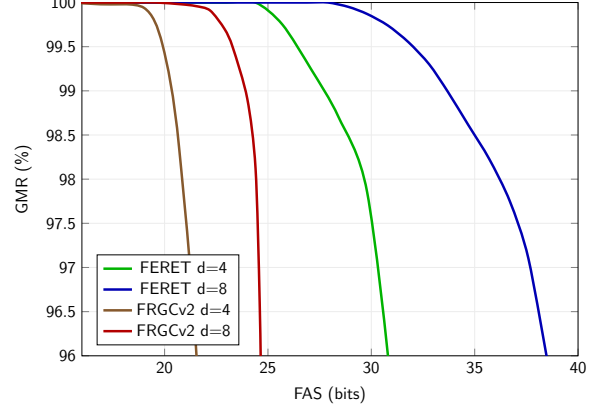


Fig. 7: Performance rates in relation to the FAS.

However, for some polynomial degrees no false matches have been observed, see table V. In such cases, the FAS can not be estimated and is approximated by linearly interpolating the FASs of the last two polynomial degrees for which the FAS could be estimated. Alternatively, other approximations, *e.g.* rule of three [83], could be applied. But the rule of three for example, does not consider the fact that security is expected to increase as  $k$  increases. Table VI summarises FASs in relation to the Genuine Match Rate (GMR=1-FNMR) provided by the fuzzy vault scheme using the Guruswami-Sudan decoding strategy (interpolated FAS values are marked italic). On the FERET database, a FASs of approximately 25 bits and 30 bits are obtained for a GMRs of 100% and 95%, respectively, in case 4 intervals are used. For the same GMRs, on the more challenging FRGCv2 database, FASs of around 20 bits and 22 bits are achieved. For the use of 8 intervals, slightly higher FASs are approximated on both databases.

Figure 7 illustrates the relation between GMR and FAS on both databases. It can be seen that the employed approximation results in steeply descending curves, thus providing a conservative approximation of the FAS for polynomial degrees where no false match is observed.

Another threat are correlation attacks that combine two or more vaults derived from the same subject. The correlation attack of [60], [61] on the original fuzzy vault scheme, which represents a special linkage attack, can not be applied to the improved fuzzy vault scheme. It has been shown in [63] that two related vaults  $V(X)$  and  $W(X)$  protecting the feature sets  $\mathbf{P}$  and  $\mathbf{P}'$ , respectively, can be attacked efficiently and effectively based on the extended Euclidean algorithm, provided that

$$|\mathbf{P} \cap \mathbf{P}'| \geq (\max(|\mathbf{P}|, |\mathbf{P}'|) + k)/2. \quad (6)$$

This attack is prevented by applying the bijection [63], *i.e.* remapping of feature elements. Due to the assumed randomness of two bijections  $\sigma$  and  $\sigma'$ , the corresponding sets  $\sigma(\mathbf{P})$  and  $\sigma'(\mathbf{P}')$  are random and, based on the definition of the hypergeometric distribution, the probability that for these sets Eq. 6 is fulfilled is equal to

$$1 - \left( \frac{\rho}{|\mathbf{P}|} \right)^{-1} \sum_{j=0}^{\omega_0-1} \binom{|\mathbf{P}'|}{j} \binom{\rho - |\mathbf{P}'|}{|\mathbf{P}| - j}, \quad (7)$$

TABLE VII: Comparison with most relevant works on face-based fuzzy vault schemes.

| Approach                   | Database  | Feature Extraction                       | Feature Transformation   | Decoding Strategy                 | Performance Rates                     | Security Rates  |
|----------------------------|---|--|--|-----------------------------------|---------------------------------------|---|
| Feng <i>et al.</i> [69]    | ORL face database (40 subjects)                         | Eigenfaces and Fisherfaces with LDA      | Quantisation of feature vector segments  | Reed Solomon                      | ~5% EER (non-stolen token scenario)   | 41 bits brute force security                                |
| Wang and Plataniotis [70]  | ORL face database                                       | Eigenfaces with PCA                      | Random transformation, feature quantisation, binarisation  | Cyclic Redundancy Check           | FNMR=0.5%, FMR=7.38%                  | ~ 57 bits brute force security                              |
| Frassen <i>et al.</i> [84] | 3D face database (100 subjects)                         | Depth-histogram-based feature extraction | Binarisation, quantisation of bit chunks with address bits                                       | Least Squares Fitting             | FNMR=4.1%, FMR=0.0%                   | ~ 90 bits brute force security                              |
| Wu and Yuan [71]           | ORL face database                                       | Eigenfaces with PCA                      | Random transformation, quantisation of feature elements  | Cyclic Redundancy Check           | FNMR=21.0%, FMR=16.5%                 | n.a.  |
| Nagar <i>et al.</i> [36]   | XM2VTS and WVU databases (100/138 subjects)             | Histogram-equalisation with LDA          | Unary encoding-based binarisation, quantisation of bit chunks                                    | Berlekamp-Massey for Reed-Solomon | FNMR=33%/42% (WVU/XM2VTS)             | 51 bits false accept security                               |
| This work                  | FERET and FRGCv2 databases (subsets) (529/533 subjects) | DCNN (ArcFace)                           | Quantisation, LSSC-based binarisation of feature elements, mapping of binary code to feature set | Guruswami-Sudan                   | <1% FNMR at <0.01% FMR (FERET/FRGCv2) | ~ 32 bits (FERET)<br>~ 24 bits (FRGC) false accept security |

where  $\omega_0 = \lceil (|\mathbf{P}| + k)/2 \rceil$ ,  $\rho = d|\mathbf{P}|$ , and w.l.o.g.  $|\mathbf{P}| \geq |\mathbf{P}'|$ . For the used feature extractor and the feature transformation this probability is negligible. Hence, the requirement of unlinkability is fulfilled.

In order to obscure the size of the vault, which might leak information about the protected deep face representation, it is suggested choose a random polynomial  $Q(X)$  of degree  $nm-t$  which should not exhibit zeros in  $\mathbf{F}$ . Subsequently,  $V(X)$  can be defined as  $V(X) = \kappa(X) + Q(X) \cdot \prod_{v \in \mathbf{P}} (X - v)$  and thereby, it will always be of degree  $nm$ .

Finally, note that a narrow distribution of feature set sizes provides a similar level of security across users where the minimum security is expected to be close to the average, *c.f.* figure 6. Note that this is usually not guaranteed for other biometric feature sets, *e.g.* minutiae sets.

In addition, table V lists the average decoding times for mated ( $t_g$ ) and non-mated ( $t_i$ ) decoding attempts (excluding the time required for feature extraction). Runtime measures were conducted on a single core of an Intel® Core™ i5-8250U CPU at 1.60 GHz. Efficient decoding times which are significantly below 100 ms are obtained for the use of 4 intervals and polynomial sizes up to 512. For 8 intervals and polynomial degrees of less than 1200, decoding times below 500 ms are achieved. That is, key retrieval can be performed in real time for relevant parameters of the proposed fuzzy vault scheme which is essential for the usability of the system.

#### E. Comparison with other Works

Table VII provides a comparison of the most relevant works against the proposed system. It can be observed that the presented fuzzy vault scheme significantly outperforms all published approaches in terms of biometric performance. It is worth noting that in contrast to the listed works, the proposed scheme is evaluated on more challenging databases.

Focusing on security in terms of BFS, the presented system would outperform published approaches by orders of magnitude. Furthermore, the FMRs reported in [69]–[71] show that

the FAS of these schemes is extremely low which confirms our assertion that BFS is not a useful measure for the actual security, *i.e.* against arbitrary attacks.

Moreover, the FAS of 51 bits in [36] is reported for unpractical FNMRs above 30% while at a GMR of 95% the FAS decreases below 22 bits. Further, it is noteworthy that the computational effort for a genuine decoding (verification) attempt in [36] is very high and increases with the security parameters; it is, thus, questionable whether this scheme is practical for higher security levels. That is, the proposed system is expected to outperforms existing face-based fuzzy vault schemes which is confirmed by the extrapolated FAS.

To the best of the authors' knowledge, the security level achieved by of our scheme is one of the highest of biometric cryptosystems based on a single biometric characteristic<sup>3</sup>. Of course, multi-biometric schemes can provide higher security levels. For instance, for the use of four fingerprints in [67] and two irises [68], a false accept security of 65 and 57 bits have been reported at a FNMR of 7%, respectively.

## V. CONCLUSION

It is well-known that biometric samples can be reconstructed from their corresponding templates [86]. In particular face images can be approximated from deep face representations using deep learning techniques [87]. Very recently, this has also been shown for binarised templates [88]. Thus, biometric template protection mechanisms are required to prevent from misuse of biometric reference data.

Focusing on face recognition, some types of template protection schemes already achieve provable security against attacks while maintaining recognition performance of unprotected systems, *e.g.* homomorphic encryption [52]. Beyond that, biometric cryptosystems offer biometric-dependent key derivation which is an essential use-case for the management

<sup>3</sup>A security of 73 bits has been achieved by a scheme based on genetic fingerprints [85], but this characteristic is not relevant for real-time applications.

of passwords and private keys. This work showed that biometric cryptosystems, in particular the fuzzy vault scheme, can be effectively applied to protect and derive digital keys from deep face representations.

The following topics could be of interest for future research:

- While this work considers a cooperative authentication scenario, the biometric performance and security of the proposed face fuzzy vault system could be evaluated on less-constrained databases, *e.g.* Labelled Faces in the Wild (LFW) [89]. If the recognition accuracy of the baseline face recognition degrades in a more challenging scenario, the biometric performance of proposed system is expected to be negatively affected, too. However, for the same parameters it may not impact the provided security since biometric sample quality generally only impact genuine comparisons and thus the FNMR of a face recognition system.
- The proposed system outperforms published works on face-based fuzzy vault schemes in terms of biometric performance, *c.f.* table VII. However, in order to provide higher security in terms of FAS, the fuzzy vault scheme could be hardened using a password or a multi-biometric fuzzy vault scheme could be constructed using further biometric characteristics, as suggested in [36]. Since the proposed transformation method can be applied to any fixed-length real valued feature vectors, an extension of this work to a multi-biometric fuzzy vault using feature-level fusion with neural networks is straightforward.
- The runtime of the employed polynomial reconstruction method might be further improved. *E.g.* in [67], it is suggested to initially apply a classical Reed-Solomon decoder to recover the correct polynomial; if unsuccessful, a Guruswami-Sudan algorithm is iteratively applied with increasing multiplicity until the correct polynomial is found or a maximum multiplicity is reached. It was shown that thereby, decoding times for mated verification attempts can be significantly decreased. A similar strategy could be used in the proposed system.

#### ACKNOWLEDGEMENTS

This research work has been partially funded by the German Federal Ministry of Education and Research and the Hessian Ministry of Higher Education, Research, Science and the Arts within their joint support of the National Research Center for Applied Cybersecurity ATHENE.

#### REFERENCES

- [1] T. Ahonen, A. Hadid, and M. Pietikainen, “Face description with local binary patterns: Application to face recognition,” *IEEE Transactions on Pattern Analysis and Machine Intelligence*, vol. 28, no. 12, pp. 2037–2041, 2006.
- [2] L. Shen, L. Bai, and M. Fairhurst, “Gabor wavelets and general discriminant analysis for face identification and verification,” *Image and Vision Computing*, vol. 25, no. 5, pp. 553 – 563, 2007.
- [3] S. Z. Li and A. K. Jain, Eds., *Handbook of Face Recognition*. Springer London, 2011.
- [4] L. Liu, J. Chen, P. Fieguth, G. Zhao, R. Chellappa, and M. Pietikäinen, “From BoW to CNN: Two Decades of Texture Representation for Texture Classification,” *International Journal of Computer Vision*, vol. 127, no. 1, pp. 74–109, 2019.
- [5] O. M. Parkhi, A. Vedaldi, and A. Zisserman, “Deep face recognition,” in *British Machine Vision Conf. (BMVC)*, 2015, pp. 41.1–41.12.
- [6] G. Guo and N. Zhang, “A survey on deep learning based face recognition,” *Computer Vision and Image Understanding*, vol. 189, p. 102805, 2019.
- [7] Y. Taigman, M. Yang, M. Ranzato, and L. Wolf, “DeepFace: Closing the Gap to Human-Level Performance in Face Verification,” in *Conf. on Computer Vision and Pattern Recognition (CVPR)*, 2014, pp. 1701–1708.
- [8] R. Ranjan, S. Sankaranarayanan, A. Bansal, N. Bodla, J. Chen, V. M. Patel, C. D. Castillo, and R. Chellappa, “Deep learning for understanding faces: Machines may be just as good, or better, than humans,” *IEEE Signal Processing Magazine*, vol. 35, no. 1, pp. 66–83, 2018.
- [9] European Parliament, “Regulation (EU) 2016/679,” *Official Journal of the European Union*, vol. L119, pp. 1–88, April 2016.
- [10] A. Cavoukian and A. Stoianov, *Biometric Encryption: The New Breed of Untraceable Biometrics*, 2010, pp. 655–718.
- [11] C. Rathgeb and A. Uhl, “A survey on biometric cryptosystems and cancelable biometrics,” *EURASIP Journal on Information Security*, vol. 2011, no. 3, 2011.
- [12] K. Nandakumar and A. K. Jain, “Biometric template protection: Bridging the performance gap between theory and practice,” *IEEE Signal Processing Magazine - Special Issue on Biometric Security and Privacy*, pp. 1–12, 2015.
- [13] ISO/IEC JTC 1/SC 27 IT Security techniques, *ISO/IEC 24745:2011. Information technology – Security techniques – Biometric information protection*, International Organization for Standardization and International Electrotechnical Committee, June 2011.
- [14] A. Juels and M. Wattenberg, “A fuzzy commitment scheme,” in *6th ACM Conf. on Computer and Communications Security (CCS)*, 1999, pp. 28–36.
- [15] A. Juels and M. Sudan, “A fuzzy vault scheme,” in *IEEE Int'l Symposium on Information Theory (ISIT)*, 2002, p. 408.
- [16] L. Ballard, S. Kamara, and M. K. Reiter, “The practical subtleties of biometric key generation,” in *17th Conference on Security Symposium (SS)*, 2008, p. 61–74.
- [17] T. Ignatenko and F. M. J. Willems, “Biometric systems: Privacy and secrecy aspects,” *IEEE Transactions on Information Forensics and Security*, vol. 4, no. 4, pp. 956–973, 2009.
- [18] A. K. Jain, K. Nandakumar, and A. Nagar, “Biometric template security,” *EURASIP Journal Adv. Signal Process*, vol. 2008, pp. 1–17, 2008.
- [19] V. M. Patel, N. K. Ratha, and R. Chellappa, “Cancelable biometrics: A review,” *IEEE Signal Processing Magazine*, vol. 32, no. 5, pp. 54–65, 2015.
- [20] U. Uludag, S. Pankanti, S. Prabhakar, and A. K. Jain, “Biometric cryptosystems: issues and challenges,” *Proc. of the IEEE*, vol. 92, no. 6, pp. 948–960, 2004.
- [21] C. Aguilar-Melchor, S. Fau, C. Fontaine, G. Gogniat, and R. Sirdey, “Recent advances in homomorphic encryption: A possible future for signal processing in the encrypted domain,” *IEEE Signal Processing Magazine*, vol. 30, no. 2, pp. 108–117, 2013.
- [22] P. Drodowski, C. Rathgeb, and C. Busch, “Computational workload in biometric identification systems: An overview,” *IET Biometrics*, vol. 8, no. 6, pp. 351–368, 2019.
- [23] A. Nagar, K. Nandakumar, and A. K. Jain, “Biometric template transformation: a security analysis,” in *Media Forensics and Security II*, vol. 7541. SPIE, 2010, pp. 237 – 251.
- [24] Y. Wang, S. Rane, S. C. Draper, and P. Ishwar, “A theoretical analysis of authentication, privacy, and reusability across secure biometric systems,” *IEEE Transactions on Information Forensics and Security*, vol. 7, no. 6, pp. 1825–1840, 2012.
- [25] K. Simoens, B. Yang, X. Zhou, F. Beato, C. Busch, E. Newton, and B. Preneel, “Criteria towards metrics for benchmarking template protection algorithms,” in *Int'l Conf. on Biometrics (ICB)*, 2012, pp. 498–505.
- [26] M. Gomez-Barrero, J. Galbally, C. Rathgeb, and C. Busch, “General framework to evaluate unlinkability in biometric template protection systems,” *IEEE Transactions on Information Forensics and Security*, vol. 13, no. 6, pp. 1406–1420, 2018.
- [27] ISO/IEC JTC1 SC37 Biometrics, *ISO/IEC 30136:2018. Information technology – Performance testing of biometric template protection*, International Organization for Standardization, 2018.
- [28] M.-H. Lim, A. B. J. Teoh, and J. Kim, “Biometric feature-type transformation: Making templates compatible for secret protection,” *IEEE Signal Processing Magazine*, vol. 32, no. 5, pp. 77–87, 2015.

[29] J. Merkle, T. Kevenaar, and U. Korte, "Multi-modal and multi-instance fusion for biometric cryptosystems," in *Int'l Conf. of Biometrics Special Interest Group (BIOSIG)*, 2012, pp. 1–6.

[30] P. Drodzowski, F. Struck, C. Rathgeb, and C. Busch, "Benchmarking binarisation schemes for deep face templates," in *Int'l Conf. on Image Processing (ICIP)*. IEEE, 2018, pp. 1–5.

[31] M. Ao and S. Z. Li, "Near infrared face based biometric key binding," in *Int'l Conf. on Biometrics (ICB)*, 2009, pp. 376–385.

[32] R. Xia, Y. Pan, H. Lai, C. Liu, and S. Yan, "Supervised hashing for image retrieval via image representation learning," in *AAAI Conf. on Artificial Intelligence*, 2014.

[33] V. E. Lioni, Jiwen Lu, Gang Wang, P. Moulin, and Jie Zhou, "Deep hashing for compact binary codes learning," in *Conf. on Computer Vision and Pattern Recognition (CVPR)*, 2015, pp. 2475–2483.

[34] V. Talreja, M. C. Valenti, and N. M. Nasrabadi, "Deep hashing for secure multimodal biometrics," *IEEE Transactions on Information Forensics and Security*, vol. 16, pp. 1306–1321, 2021.

[35] G. Mai, K. Cao, X. Lan, and P. C. Yuen, "Secureface: Face template protection," *IEEE Transactions on Information Forensics and Security*, vol. 16, pp. 262–277, 2021.

[36] A. Nagar, K. Nandakumar, and A. Jain, "Multibiometric cryptosystems based on feature-level fusion," *Trans. on Information Forensics and Security*, vol. 7, no. 1, pp. 255–268, 2012.

[37] N. Ratha, J. Connell, and R. Bolle, "Enhancing security and privacy in biometrics-based authentication systems," *IBM Systems Journal*, vol. 40, no. 3, pp. 614–634, 2001.

[38] M. Savvides, B. V. K. Vijaya Kumar, and P. K. Khosla, "Cancelable biometric filters for face recognition," in *17th Int'l Conf. on Pattern Recognition (ICPR)*, 2004, pp. 922–925.

[39] A. B. J. Teoh, A. Goh, and D. C. L. Ngo, "Random multispace quantization as an analytic mechanism for biohashing of biometric and random identity inputs," *IEEE Transactions on Pattern Analysis and Machine Intelligence*, vol. 28, no. 12, pp. 1892–1901, 2006.

[40] T. Boult, "Robust distance measures for face-recognition supporting revocable biometric tokens," in *Int'l Conf. on Automatic Face and Gesture Recognition (FGFR)*, 2006, pp. 560–566.

[41] M. Gomez-Barrero, C. Rathgeb, J. Galbally, C. Busch, and J. Fierrez, "Unlinkable and irreversible biometric template protection based on bloom filters," *Information Sciences*, vol. 370–371, pp. 18–32, 2016.

[42] A. Kong, K.-H. Cheung, D. Zhang, M. Kamel, and J. You, "An analysis of biohashing and its variants," *Pattern Recognition*, vol. 39, no. 7, pp. 1359 – 1368, 2006.

[43] J. Bringer, C. Morel, and C. Rathgeb, "Security analysis and improvement of some biometric protected templates based on bloom filters," *Image and Vision Computing*, vol. 58, pp. 239 – 253, 2017.

[44] L. Ghammam, K. Karabina, P. Lacharme, and K. Thiry-Atighehchi, "A cryptanalysis of two cancelable biometric schemes based on index-of-max hashing," *IEEE Transactions on Information Forensics and Security*, vol. 15, pp. 2869–2880, 2020.

[45] S. Kirchgasser, Y. M. Diaz, H. Mendez-Vazquez, and A. Uhl, "Is warping-based cancellable biometrics (still) sensible for face recognition?" in *Int'l Joint Conference on Biometrics (IJCB)*, 2020, pp. 1–8.

[46] A. B. Teoh, D. C. Ngo, and A. Goh, "Personalised cryptographic key generation based on facehashing," *Computers & Security*, vol. 23, no. 7, pp. 606 – 614, 2004.

[47] M. van der Veen, T. Kevenaar, G.-J. Schrijen, T. H. Akkermans, and F. Zuo, "Face biometrics with renewable templates," in *Security, Steganography, and Watermarking of Multimedia Contents VIII*, vol. 6072. SPIE, 2006, pp. 205 – 216.

[48] B. Tams, "Decodability attack against the fuzzy commitment scheme with public feature transforms," 2014. [Online]. Available: <http://arxiv.org/abs/1406.1154>

[49] V. N. Boddeti, "Secure face matching using fully homomorphic encryption," in *Int'l Conf. on Biometrics Theory, Applications and Systems (BTAS)*, 2019, pp. 1–10.

[50] P. Drodzowski, N. Buchmann, C. Rathgeb, M. Margraf, and C. Busch, "On the application of homomorphic encryption to face identification," in *Int'l Conf. of the Biometrics Special Interest Group (BIOSIG)*, 2019, pp. 1–8.

[51] J. J. Engelsma, A. K. Jain, and V. N. Boddeti, "HERS: Homomorphically encrypted representation search," *arXiv*, 2020. [Online]. Available: <https://arxiv.org/abs/2003.12197>

[52] J. Kolberg, P. Drodzowski, M. Gomez-Barrero, C. Rathgeb, and C. Busch, "Efficiency analysis of post-quantum-secure face template protection schemes based on homomorphic encryption," in *Int'l Conf. of the Biometrics Special Interest Group (BIOSIG)*, 2020, pp. 1–4.

[53] A. Morales, J. Fierrez, R. Vera-Rodriguez, and R. Tolosana, "SensitiveNets: Learning agnostic representations with application to face images," *IEEE Transactions on Pattern Analysis and Machine Intelligence*, pp. 1–8, 2020.

[54] P. Terhört, K. Riehl, N. Damer, P. Rot, B. Bortolato, F. Kirchbuchner, V. Struc, and A. Kuijper, "PE-MIU: A training-free privacy-enhancing face recognition approach based on minimum information units," *IEEE Access*, vol. 8, pp. 93 635–93 647, 2020.

[55] A. Juels and M. Sudan, "A fuzzy vault scheme," *Designs, Codes and Cryptography*, vol. 38, no. 2, pp. 237–257, 2006.

[56] T. C. Clancy, N. Kiyavash, and D. J. Lin, "Secure smartcard-based fingerprint authentication," in *SIGMM workshop on Biometrics methods and applications (WBMA)*, 2003, pp. 45–52.

[57] K. Nandakumar, A. K. Jain, and S. Pankanti, "Fingerprint-based fuzzy vault: Implementation and performance," *IEEE Trans. Information Information Forensics and Security*, vol. 2, no. 4, pp. 744–757, 2007.

[58] A. Nagar, K. Nandakumar, and A. K. Jain, "A hybrid biometric cryptosystem for securing fingerprint minutiae templates," *Pattern Recogn. Lett.*, vol. 31, pp. 733–741, 2010.

[59] V. Krivokucu, W. H. Abdulla, and A. Swain, "A dissection of fingerprint fuzzy vault schemes," in *Image and Vision Computing New Zealand (IVCNZ)*, 2012, pp. 256–261.

[60] W. J. Scheirer and T. E. Boult, "Cracking fuzzy vaults and biometric encryption," in *Biometrics Symposium*, 2007, pp. 1–6.

[61] A. Kholmatov and B. Yanikoglu, "Realization of correlation attack against the fuzzy vault scheme," in *Security, Forensics, Steganography, and Watermarking of Multimedia Contents X*, vol. 6819. SPIE, 2008.

[62] Y. Dodis, R. Ostrovsky, L. Reyzin, and A. Smith, "Fuzzy extractors: How to generate strong keys from biometrics and other noisy data," *SIAM Journal on Computing*, vol. 38, no. 1, pp. 97–139, 2008.

[63] J. Merkle and B. Tams, "Security of the improved fuzzy vault scheme in the presence of record multiplicity (full version)," *arXiv*, 2013. [Online]. Available: <http://arxiv.org/abs/1312.5225>

[64] B. Tams, P. Mihăilescu, and A. Munk, "Security considerations in minutiae-based fuzzy vaults," *IEEE Trans. Information Information Forensics and Security*, vol. 10, no. 5, pp. 985–998, 2015.

[65] Y. J. Lee, K. Bae, S. J. Lee, K. R. Park, and J. Kim, "Biometric key binding: Fuzzy vault based on iris images," in *Int'l Conf. on Biometrics (ICB)*, 2007, pp. 800–808.

[66] W. Ponce-Hernandez, R. Blanco-Gonzalo, J. Liu-Jimenez, and R. Sanchez-Reillo, "Fuzzy vault scheme based on fixed-length templates applied to dynamic signature verification," *IEEE Access*, vol. 8, pp. 11 152–11 164, 2020.

[67] B. Tams, "Unlinkable minutiae-based fuzzy vault for multiple fingerprints," *IET Biometrics*, vol. 5, pp. 170–180, 2016.

[68] C. Rathgeb, B. Tams, J. Wagner, and C. Busch, "Unlinkable improved multi-biometric iris fuzzy vault," *EURASIP Journal on Information Security*, vol. 2016, no. 1, p. 26, 2016.

[69] Y. C. Feng and P. C. Yuen, "Protecting face biometric data on smartcard with reed-solomon code," in *Conference on Computer Vision and Pattern Recognition Workshop (CVPRW)*, 2006, pp. 29–29.

[70] Y. Wang and K. N. Plataniotis, "Fuzzy vault for face based cryptographic key generation," in *Biometrics Symposium*, 2007, pp. 1–6.

[71] L. Wu and S. Yuan, "A face based fuzzy vault scheme for secure online authentication," in *2nd International Symposium on Data, Privacy, and E-Commerce (ISDPE)*, 2010, pp. 45–49.

[72] S. Gao, "A new algorithm for decoding reed-solomon codes," in *Communications, Information and Network Security*, 2002, pp. 55–68.

[73] V. Guruswami and M. Sudan, "Improved decoding of reed-solomon and algebraic-geometric codes," *IEEE Transactions on Information Theory*, vol. 45, pp. 1757–1767, 1998.

[74] F. Gray, "Pulse code communications," 1953, u.S. Patent 2,632,058.

[75] M.-H. Lim and A. B. J. Teoh, "A novel encoding scheme for effective biometric discretization: Linearly separable subcode," *IEEE Transactions on Pattern Analysis and Machine Intelligence*, vol. 35, no. 2, pp. 300–313, 2013.

[76] J. Deng, J. Guo, N. Xue, and S. Zafeiriou, "ArcFace: Additive angular margin loss for deep face recognition," in *Conf. on Computer Vision and Pattern Recognition (CVPR)*, 2019, pp. 4685–4694.

[77] D. E. King, "Dlib-ml: A machine learning toolkit," *The Journal of Machine Learning Research*, vol. 10, pp. 1755–1758, 2009.

[78] P. Phillips, H. Wechsler, J. Huang, and P. J. Rauss, "The FERET database and evaluation procedure for face-recognition algorithms," *Image and Vision Computing*, vol. 16, no. 5, pp. 295–306, 1998.

[79] P. Phillips, P. Flynn, T. Scruggs, K. Bowyer, J. Chang, K. Hoffman, J. Marques, J. Min, and W. Worek, "Overview of the face recognition

grand challenge,” in *Conf. on Computer Vision and Pattern Recognition (CVPR)*, 2005.

[80] International Civil Aviation Organization, “Machine readable passports – part 9 – deployment of biometric identification and electronic storage of data in eMRTDs,” International Civil Aviation Organization (ICAO), 2015.

[81] ISO/IEC JTC1 SC37 Biometrics, *ISO/IEC 19795-1:2006. Information Technology – Biometric Performance Testing and Reporting – Part 1: Principles and Framework*, International Organization for Standardization and International Electrotechnical Committee, April 2006.

[82] J. Daugman, “Biometric decision landscapes,” University of Cambridge - Computer Laboratory, Tech. Rep. UCAM-CL-TR-482, 2000.

[83] ISO/IEC TC JTC1 SC37 Biometrics, *ISO/IEC 19795-1:2006. Information Technology – Biometric Performance Testing and Reporting – Part 1: Principles and Framework*, International Organization for Standardization and International Electrotechnical Committee, Mar. 2006.

[84] T. Frassen, X. Zhou, and C. Busch, “Fuzzy vault for 3d face recognition systems,” in *Int'l Conf. on Intelligent Information Hiding and Multimedia Signal Processing (IIH-MSP)*, 2008, pp. 1069–1074.

[85] U. Korte, M. Krawczak, J. Merkle, R. Plaga, M. Niesing, C. Tiemann, H. Vinck, and U. Martini, “A cryptographic biometric authentication system based on genetic fingerprints,” in *Sicherheit, Schutz und Zuverlässigkeit (SICHERHEIT)*, 2008, pp. 263–276.

[86] M. Gomez-Barrero and J. Galbally, “Reversing the irreversible: A survey on inverse biometrics,” *Computers & Security*, vol. 90, p. 101700, 2020.

[87] G. Mai, K. Cao, P. C. Yuen, and A. K. Jain, “On the reconstruction of face images from deep face templates,” *IEEE Transactions on Pattern Analysis and Machine Intelligence*, vol. 41, no. 5, pp. 1188–1202, 2019.

[88] D. Keller, M. Osadchy, and O. Dunkelman, “Fuzzy commitments offer insufficient protection to biometric templates produced by deep learning,” 2020. [Online]. Available: <https://arxiv.org/abs/2012.13293>

[89] E. Learned-Miller, G. B. Huang, A. RoyChowdhury, H. Li, , and G. Hua, “Labeled faces in the wild: A survey,” in *Advances in Face Detection and Facial Image Analysis*. Springer, 2016, pp. 189–248.